crystals

MDPI

Communication

Self-Assembly of a Carboxyl-Functionalized BODIPY Dye via Hydrogen Bonding

Beatriz Matarranz, Angel Sampedro, Constantin G. Daniliuc and Gustavo Fernández *

Organisch-Chemisches Institut, Westfälische Wilhelms-Universität Münster, Corrensstraße, 40, 48149 Münster, Germany; matarran@uni-muenster.de (B.M.); sampedropalermangel@gmail.com (A.S.); constantin.daniliuc@wwu.de (C.G.D.)

* Correspondence: fernandg@uni-muenster.de

Received: 19 October 2018; Accepted: 16 November 2018; Published: 20 November 2018

Abstract: We report the synthesis, characterization, and self-assembly behavior of a 4,4-Difluoro-4-bora-3a,4a-diaza-*s*-indacene (BODIPY) dye functionalized at the *meso*-position with a butyric acid group. Various spectroscopic investigations (UV-Vis, emission, and Fourier-transform infrared spectroscopy (FTIR) studies) supported by X-ray analysis revealed the formation of self-assembled structures in the solid state with translationally stacked BODIPY units driven by hydrogen bonding between the carboxyl groups.

Keywords: BODIPY dyes; hydrogen bonding; Self-Assembly; weak non-covalent interactions

1. Introduction

4,4-Difluoro-4-bora-3a,4a-diaza-*s*-indacene (BODIPY) dyes are a well-known class of functional dyes with superior optical, photophysical, and electronic properties [1,2]. The planar and sterically accessible nature of the BODIPY core anticipates its involvement in non-covalent interactions via stacking of the dipyrromethene core. In contrast to other multiple classes of organic dyes and π-conjugated molecules, the supramolecular chemistry of BODIPY dyes has remained considerably less explored. The past 10–15 years, however, have witnessed an increasing interest in the design and construction of self-assembled structures, mesophases, and solid-state materials based on BODIPY dyes. A recent review by Ajayaghosh and co-workers nicely illustrates the developments in the field [3]. For instance, examples of BODIPY-based liquid crystals [4,5], nanoparticle assemblies [6–8], mechanically-driven Near-Infrared (NIR) emitters [9], and supramolecular polymers [10–12] have been reported. A particularly interesting approach is the introduction of hydrogen bonding units that can operate orthogonally to stacking interactions [13,14], which often results in ordered supramolecular structures. In this regard, our group has recently shown that amide groups can, indeed, increase the stability of supramolecular assemblies of BODIPY dyes both in nonpolar [15] and aqueous media [16,17] via cooperative hydrogen bonding interactions.

In this manuscript, we examine the influence of carboxyl groups on the self-assembly behavior of BODIPY dyes in the solid state. For this purpose, we have investigated a BODIPY dye substituted with a butyric acid residue at the *meso* position (compound **1** in Scheme 1). We envisaged that this relatively bulky substituent may induce the formation of emissive assemblies *via* the formation of translationally slipped π-stacks, whereas dimerization of the carboxyl groups are expected to further stabilize the assembly *via* intermolecular hydrogen bonds.

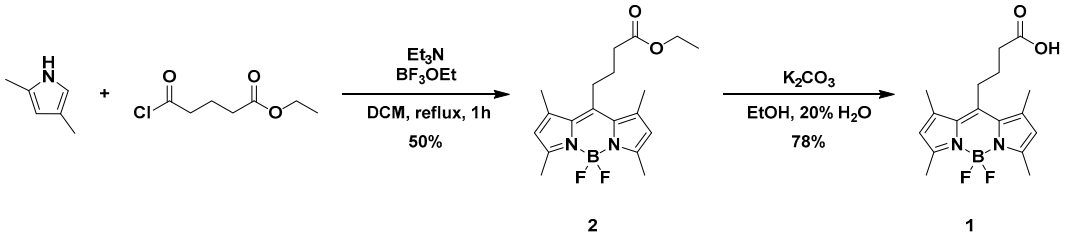

Scheme 1. Synthesis of compound **1**.

2. Experimental Section

2.1. Materials and Methods

All chemicals were purchased from Sigma-Aldrich (St. Louis, MO, USA), TCI Europe N.V. (Tokyo, Japan) or Alfa Aesar (Ward Hill, MA, USA) and used without further purification. Dichloromethane was first pre-dried over $CaCl_2$ and then distilled over P_2O_5 under argon atmosphere. ^{1}H-NMR spectra were recorded on an Agilent DD2 600 at 298 K using partially deuterated solvents as internal standards. Coupling constants (*J*) are denoted in Hz and chemical shifts (δ) in ppm. Multiplicities are denoted as follows: s = singlet, d = doublet, t = triplet, m = multiplet. Chemical shifts are given in ppm relative to TMS (^{1}H, 0.0 ppm). UV/Vis absorption spectra were recorded on a Jasco V-770 (JASCO, Tokio, Japan) or a Jasco V-750 (JASCO, Tokio, Japan) spectrophotometers, both equipped with peltier cells and Julabo F250 (JULABO GmbH, Seelbach, Germany) water circulation units. Fluorescence spectra were recorded on a Jasco FP-8500 (JASCO, Tokio, Japan) spectrofluorometer equipped with the same water circulation unit. Infrared spectra were measured on a Jasco FTIR-4600LE (JASCO, Tokio, Japan).

2.2. Synthesis

Compounds **1** and **2** were prepared according to previously reported literature procedures and showed identical properties to those reported herein [17].

2.2.1. Synthesis of Compound **2**

In a 250 mL round bottom flask, glutaric acid monoethyl ester chloride (3.2 mL, 22 mmol) was added and dissolved in dry CH_2Cl_2 (50 mL). After cooling the solution to 0 °C, 2,4-dimethylpyrrole (5.0 mL, 47.6 mmol) was added dropwise under argon atmosphere. Afterwards, the darker solution was stirred for 20 min at 0 °C and additional 30 min at room temperature. The solution was subsequently cooled to 0 °C in an ice-bath and distilled Et_3N (9.25 mL, 66 mmol) was then added slowly and stirred at room temperature for 15 min. After that, $BF_3{\cdot}OEt_2$ (13.7 mL, 110 mmol) was added portionwise and the reaction mixture stirred overnight at room temperature under dark conditions. After 18 h, the solution was diluted with H_2O (60 mL) and stirred for two hours. The organic phase was subsequently washed with H_2O (3 × 50 mL) and brine (2 × 50 mL), dried over Na_2SO_4 and concentrated under reduced pressure to obtain an orange solid. The crude product was next dissolved in a small amount of CH_2Cl_2 and filtered through a short silica gel pad, obtaining a reddish solution that was concentrated to obtain an orange solid. This solid was finally washed with cold EtOH to obtain product **2** as orange needles (3.991 g, Yield: 50%). **^{1}H-NMR** (600 MHz, $CDCl_3$) δ: 6.06 (s, 2H), 4.15 (q, $^3J_{H,H}$ = 7.1 Hz, 2H), 3.00 (m, 2H), 2.51 (s, 6H), 2.49 (t, $^3J_{H,H}$ = 7.2 Hz, 2H), 2.43 (s, 6H), 1.96 (m, 2H), 1.27 (t, $^3J_{H,H}$ = 7.1 Hz, 3H). **^{13}C-NMR** (151 MHz, $CDCl_3$) δ: 172.66, 154.31, 145.19, 140.55, 131.60, 121.92, 60.81, 34.57, 27.66, 27.00, 16.51, 14.62, 14.38.

2.2.2. Synthesis of Compound **1**

Compound **2** (2.00 g, 5.5 mmol) and K_2CO_3 (6.05 g, 43.4 mmol) were added to a 250 mL round bottom flask and diluted with EtOH (150 mL) and H_2O (37 mL), obtaining a suspension which was stirred overnight protected from light at 50 °C. The reaction control *via* thin layer chromatography

showed the consumption of the starting material and the solvent was removed under reduced pressure, obtaining an orange precipitate when most of the alcohol was removed. This suspension was then diluted with H_2O and rinsed with CH_2Cl_2 until no major fluorescence was observed in the extracts. The resulting aqueous solution was slowly acidified until pH 3 and the product extracted with AcOEt (5 × 50 mL). The organic phase was finally washed with 0.1 M HCl (3 × 50 mL) and brine (50 mL), dried over Na_2SO_4 and concentrated to dryness to obtain compound **1** as a crystalline orange solid (1.44 g, Yield: 78%).**^{1}H-NMR** (298 K, 600 MHz, DMSO-d_6) δ 12.25 (s, 1H (OH)), 6.23 (s, 2H), 3.06–2.85 (m, 2H), 2.44–2.39 (m, 14H (BODIPY Methyl-groups (14H) + CH_2 chain (2H)), 1.84–1.73 (m, 2H). **^{13}C-NMR** (298 K, 150 MHz, DMSO-d_6) δ 174.22, 153.67, 146.50, 141.44, 131.23, 122.20, 34.19, 27.50, 27.15, 16.25, 14.52.

2.3. Crystal Structure Determination of Compound **1**

Data sets for compound **1** were collected with a Bruker APEX II CCD diffractometer. Programs used: data collection: APEX3 V2016.1-0 (Bruker AXS Inc., Madison, WI, USA, 2016); cell refinement: SAINT V8.37A (Bruker AXS Inc., Madison, WI, USA, **2015**); data reduction: SAINT V8.37A (Bruker AXS Inc., Madison, WI, USA, 2015); absorption correction, SADABS V2014/7 (Bruker AXS Inc., Madison, WI, USA, 2014); structure solution SHELXT-2015 [18]; structure refinement SHELXL-2015 [18] and graphics XP in SHELXTL [19]. *R*-values are given for observed reflections, and wR^2 values are given for all reflections. Information about the crystallographic parameters and the structure refinement is provided in Table 1. The X-ray structure of **1** has been deposited as a CIF file in the CSD database (CCDC number 1874183).

Table 1. Crystal data and structure refinement parameters for compound **1**.

Empirical Formula	**$C_{17}H_{21}BF_2N_2O{\cdot}CH_2Cl_2$**
Formula weight	419.09
Temperature/K	100(2)
Wavelength/Å	1.54178
Crystal system	Monoclinic
Space group	*C*2/*c*
Unit cell dimensions	
a/Å	27.4033(11)
b/Å	12.5495(5)
c/Å	12.3648(5)
α/°	90
β/°	110.442(2)
γ/°	90
V/Å^3	3984.4(3)
Z	8
D_c/gcm^{-3}	1.397
μ/mm^{-1}	3.234
F (000)	1.744
Crystal size/mm	0.020 × 0.160 × 0.200
θ range/°	3.92–66.74
Index ranges	$-32 \leq h \leq 32$
	$-14 \leq k \leq 14$
	$-14 \leq l \leq 14$
Reflections collected	35,692
Independent reflections	3520
R int	0.0373
Data/Restraints/Parameters	3520/0/252
GOF	1.035
Final R indexes [I > 2σ(I)]	R_1 = 0.0324
	ωR_2 = 0.0816
Final R indexes (all data)	R_1 = 0.0348
	ωR_2 = 0.0830
Largest diff. peak/hole/eÅ^{-3}	0.375/−0.413

3. Results and Discussion

3.1. UV/Vis Experiments

Solvent-dependent UV/Vis studies were initially carried out to test the ability of compound **1** to form supramolecular aggregates in solution. Figure 1 shows the absorption spectra of **1** in different solvents (c = 1 × 10^{-5} M) at room temperature. These spectra reveal sharp transitions with a common maximum between 495 and 505 nm that corresponds to the $S_0 \rightarrow S_1$ (π-π^*) transition of the BODIPY chromophore, whereas the $S_0 \rightarrow S_2$ transition appears in the region around 360–400 nm. These spectroscopic features are reminiscent to those observed for a structurally related Capsaicin-BODIPY dye recently reported by our group [17] and indicate that **1** remains as monomeric species in all investigated solvents. The molar absorption coefficients (ε) at the absorption maximum are very similar in all solvents with the exception of $CHCl_3$ and CCl_4, in which a slight red-shift and drop in the absorbance (ca. 30%) are observed. This behavior suggests the initial stages of an aggregation process, which, however, ultimately results in precipitation only after a few minutes. The limited solubility of **1** in nonpolar, i.e., alkane solvents (in which a stronger aggregation is expected), precludes a detailed analysis of the self-assembly mechanism and their corresponding thermodynamic parameters. The quantum yields of **1** (c = 1 × 10^{-6} M, absorption [a.u. < 0.1]) were measured using fluorescein as a reference (λ_{exc} = 460 nm). An overview of the emission and optical properties of **1** in different solvents is summarized in Table 2.

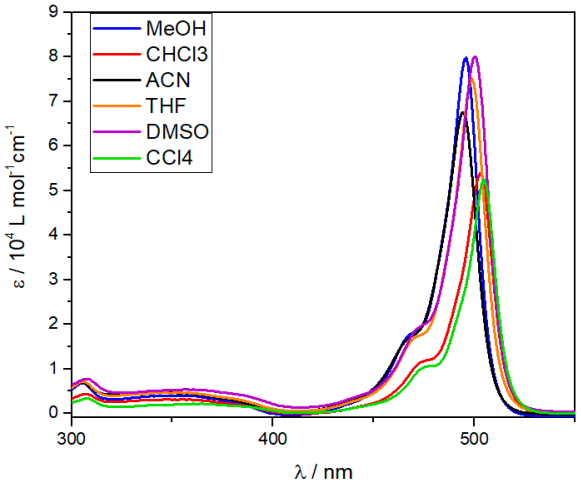

Figure 1. Solvent-dependent UV/Vis studies of compound **1** (c = 1 × 10^{-5} M, 298 K).

Table 2. Photophysical properties of compound **1** in different solvents. (c = 1 x 10^{-5} M, 298 K, λ_{exc} = 460 nm).

Solvent	λ_{abs}/nm $S_0 \rightarrow S_1$	ε/10^4 M^{-1}·cm^{-1}	λ_{em}/nm	Φ_F
MeOH	496	7.98	506	12%
DMSO	500	8.01	511	79%
THF	499	7.50	510	17%
MeCN	494	6.75	505	55%
$CHCl_3$	503	5.38	513	8%
CCl_4	505	5.24	513	14%

3.2. Solid State UV/Vis and Fluorescence Spectra

Solid-state UV-Vis and emission experiments were performed to complement the results in solution (Figure 2). MeOH was selected as solvent to prepare thin films due to the very good solubility of **1** in this medium even at high (mM) concentrations. To this end, 60 µL of a solution of **1** in MeOH (c = 1 × 10^{-3} M) were drop cast on a quartz plate until the solvent was evaporated and then absorption and emission spectra were recorded. Comparison of the absorption spectra in MeOH solution (A = 0.80 a.u.) and on thin film (A = 0.38 a.u.) reveals a broad and slightly red-shifted

absorption band ($\Delta\lambda$ = 17 nm) with a maximum at 512 nm and a shoulder at 492 nm for the latter. These features suggest the formation of an aggregate species via stacking of the BODIPY dyes in the solid state. Regarding the photoluminescence studies, **1** still shows fluorescence in the powder form and the emission maximum (545 nm) is 32 nm red-shifted compared to the molecularly dissolved state in MeOH solution. The overall spectral signatures suggest a self-assembly process via a J-type exciton coupling of the dye molecules [20].

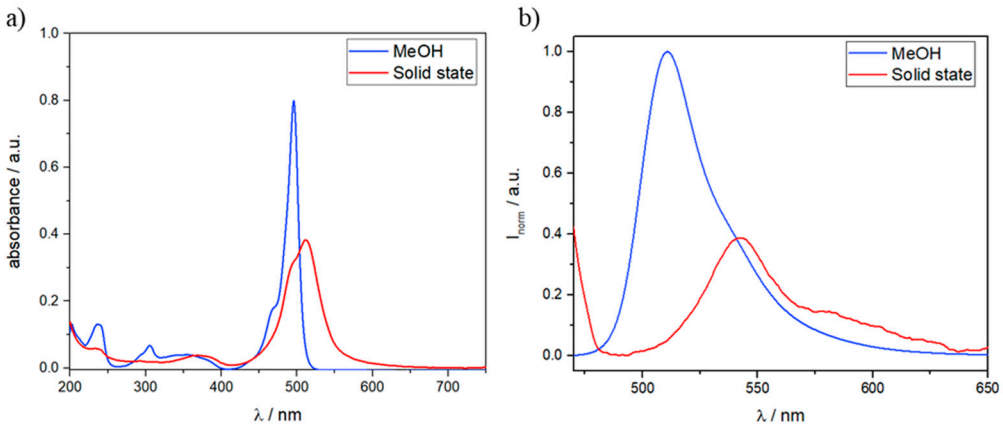

Figure 2. UV/Vis absorption (**a**) and emission (**b**) spectra of compound **1** in MeOH (c = 1 × 10^{-5} M) and in thin films from MeOH at 298 K (λ_{exc} = 450 nm).

3.3. FTIR Spectra

To examine whether intermolecular hydrogen bonding between the carboxyl groups are also involved in the aggregation of **1**, Fourier-transform infrared spectroscopy (FTIR) spectra have been recorded. Figure 3 shows a comparison of the FTIR spectra of **1** in a molecularly dissolved state (in Tetrahydrofuran (THF))- and in the aggregated state (prepared as thin film). For the thin film, the O–H stretching band appears at 3350 cm^{-1}, while this band appears at considerably higher wavenumbers (3580 cm^{-1}) for the THF solution. This behavior is attributable to the existence of hydrogen-bonded OH groups only in the film [21] whereas these groups are non-bonded in THF. On the other hand, the C=O stretching band (1736 cm^{-1}) in THF is assigned to the free C=O, while a second C=O stretching band at 1716 cm^{-1} indicates the presence of partially hydrogen-bonded C=O groups, most likely as a result of the interaction of compound **1** with the solvent molecules [22,23]. In sharp contrast, only one C=O stretching band at 1708 cm^{-1} is observed in the solid state, indicating the formation of dimers of **1** through hydrogen bonding interactions between the C=O group from one molecule and the O-H group of another one.

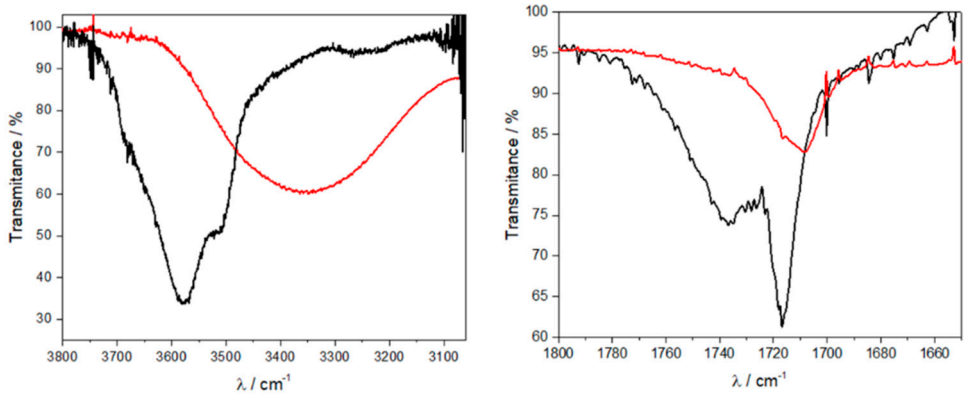

Figure 3. Fourier-transform infrared spectroscopy (FTIR) spectra of **1** in THF and in the solid state showing the O–H (**left**) and C=O (**right**) regions.

3.4. Crystal Structure of Compound **1**

By slow evaporation of a solution of **1** in DCM, orange single crystals suitable for X-ray diffraction were obtained. The crystal structure and the atom-numbering are shown in Figure 4. The crystallographic data revealed that the title compound crystallizes in the monoclinic system, space group *C*2/*c*. The central six-membered ring of the BODIPY moiety is almost coplanar with the adjacent pyrrole rings, as often observed for this class of dyes. The average bond lengths for B–N and B–F are 1.540(2) and 1.398(2) Å, and the N–B–N and F–B–F angles are 106.9(1)° and 108.8(1)°, respectively. The two B–N distances are similar, indicating the expected delocalization of the positive charge. The π-electron delocalization in the BODIPY core is confirmed by the average bond length of 1.405(2) Å. For N1–C1 and N2–C9 the found bond lengths are 1.352(2) and 1.348(2) Å, which have a pronounced double bond character.

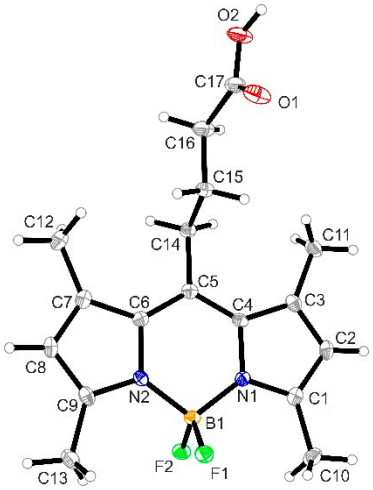

Figure 4. Crystal structure of compound **1** found in the asymmetric unit. Thermals ellipsoids are shown with 50% probability. The CH_2Cl_2 solvent molecule was omitted for clarity.

In good correlation with FTIR results, the crystal packing of compound **1** is stabilized by intermolecular hydrogen bonding involving the carboxyl groups of two molecules (dimer formation via O2–H1···O1 2.629(2) Å; 175.0(3)° interactions) and two C–H···F hydrogen bonding interactions from the cocrystallized CH_2Cl_2 molecules (C21–H21A···F2 3.129(2) Å; 141.0°; C21–H21B···F1 3.198(2) Å; 126.0°, see Figure 5a). Additionally, C–H···O interactions (C16–H16B···O2 3.430(2) Å; 138.2°), as well as C–H···F interactions (C8–H8···F1 3.362(2) Å; 142.9°), further stabilize a lateral growth of the structure in a zig-zag fashion along the *c*-axis (Figure 5b). An overview of the non-covalent interactions present in the crystal packing is summarized in Table 3.

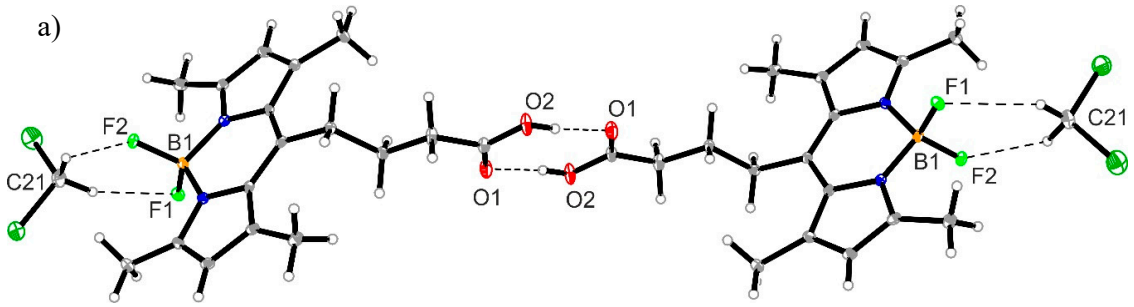

Figure 5. *Cont.*

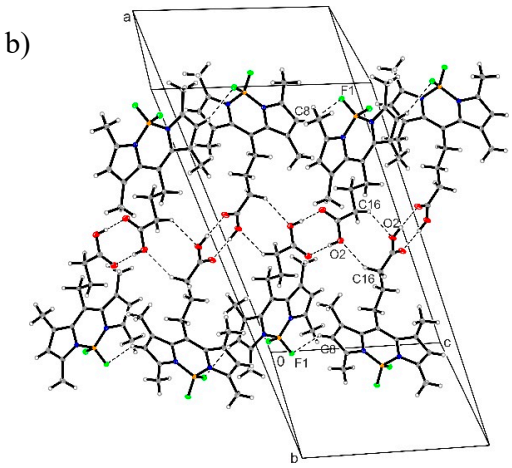

Figure 5. (**a**) Dimer formation through O–H···O hydrogen bonds between the carboxyl groups in compound **1** and additional C–H···F hydrogen bonding interactions from the cocrystallized CH_2Cl_2 molecules; (**b**) Excerpt of the packing diagram of **1** presenting the zig-zag chain formation along the *c*-axis stabilized by additional C–H···O and C–H···F interactions.

Table 3. Non-covalent intermolecular interactions in compound **1** (Å and deg) [a].

D–H···*A*	*d*(*D*–H)	*d*(H–*A*)	*d*(*D*···*A*)	∠(*D*H*A*)
O2–H1···O1$^{\#1}$	0.87(3)	1.76(3)	2.629(2)	175.0(3)
C8–H8···F1$^{\#2}$	0.95	2.55	3.362(2)	142.9
C21–H21A···F2	0.99	2.30	3.129(2)	141.0
C21–H21B···F1	0.99	2.51	3.198(2)	126.0
C12–H21B···N1$^{\#3}$	0.98	2.73	3.662(3)	157.7
C14–H14A···F2$^{\#3}$	0.99	2.56	3.383(3)	140.8
C16–H16B···O2$^{\#4}$	0.99	2.63	3.430(2)	138.2
*Cg*1···*Cg*1$^{\#3,\,a}$			3.523	

Symmetry transformations used to generate equivalent atoms: $^{\#1}$ −x, 1 − y, −z; $^{\#2}$ x, 1 − y, 0.5 + z; $^{\#3}$ 0.5 − x, 0.5 − y, 1 − z; $^{\#4}$ −x, y, 0.5 − z; [a] Cg1 is the centroid involving part of the chromophore unit: C4/C5/C6/C7/C12/N2.

Additionally to the hydrogen bonds between the carboxyl groups, intermolecular stacking of the BODIPY cores allows further growth of the dimeric units in a 2D network (Figure 6). As usually observed in crystal structures of BODIPY dyes, the BF_2 groups of stacked BODIPY units are antiparallel oriented and pointing in different directions. The stacking of the BODIPY cores does not occur in a perfect face-to-face fashion, but rather a slight translational displacement along the x and y axes is observed (Figure 6). This is most likely due to the presence of relatively bulky groups at the *meso* position, which hinders an ideal parallel organization [24,25] and results in different C21–H21B···F1, C12–H21B···N1, and C14–H14A···F2 intermolecular interactions (Figure 6a). In the 2D network, the plane formed by one BODIPY dimer is almost orthogonal to another dimer plane with a dihedral angle between both planes of 69°. Additionally, the slip angle between stacked BODIPY dyes corresponds to 29.3°, which matches well with the results obtained from spectroscopic investigations.

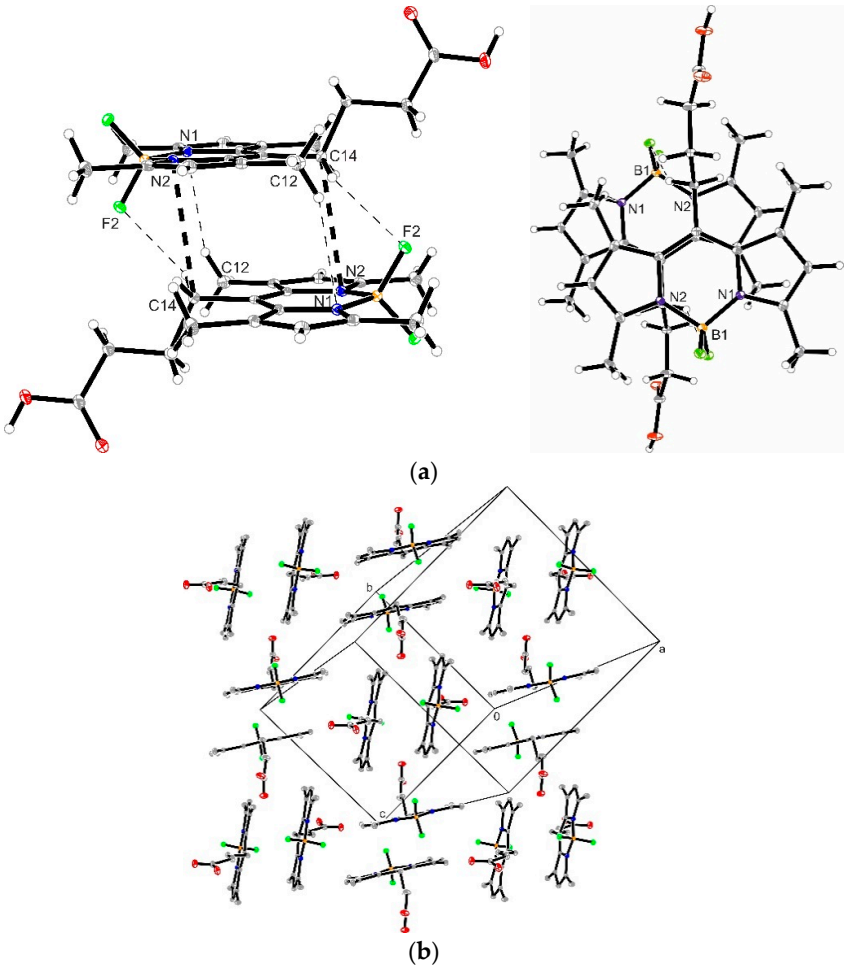

Figure 6. (**a**) View representing the interactions ($\pi\cdots\pi$, C–H$\cdots$N and C–H$\cdots$F) between two BODIPY units in compound **1**; (**b**) 2D network showing the packing of BODIPY dimeric units.

4. Conclusions

In conclusion, we investigated the self-assembly behavior of a BODIPY dye with a butyric acid residue at the *meso* position. UV/Vis, fluorescence, and FTIR experiments revealed that the target compound forms supramolecular aggregates through π-π stacking and hydrogen bonding interactions in the solid state. The molecular packing of BODIPY derivative **1** was investigated by X-ray diffraction. Dimerization of the carboxyl groups via HO–C=O$\cdots$OH–C=O intermolecular hydrogen bonding interactions combined with C–H$\cdots$F hydrogen bonding interactions from the cocrystallized CH_2Cl_2 molecules induce the growth of the structure in one dimension in a zig-zag fashion. In addition, intermolecular π-π interactions between the BODIPY cores lead to a 2D network in which the BODIPY moieties adopt a slightly slipped arrangement along both x and y axes. Our results reveal that a combination of aromatic interactions and hydrogen bonding involving carboxyl groups is a promising strategy to create stable supramolecular structures based on BODIPY dyes.

Author Contributions: Conceptualization, A.S. and G.F.; methodology, B.M., A.S. and C.G.D.; software, B.M., C.G.D. and G.F.; validation, B.M., C.G.D. and G.F.; formal analysis, B.M., C.G.D. and G.F.; investigation, A.S., B.M. and C.G.D.; writing—original draft preparation, B.M., C.G.D. and G.F.; writing—review and editing, B.M., A.S., C.G.D. and G.F.; supervision, G.F.; project administration, G.F.; funding acquisition, G.F.

Funding: This research was funded by the Deutsche Forschungsgemeinschaft (DFG), Sonderforschungsbereich (SFB) 858: Synergistic Effects in Chemistry—From Additivity towards Cooperativity.

Conflicts of Interest: The authors declare no conflict of interest. The funders had no role in the design of the study; in the collection, analyses, or interpretation of data; in the writing of the manuscript, or in the decision to publish the results.

References

1. Fan, G.; Yang, L.; Chen, Z. Water-soluble BODIPY and aza-BODIPY dyes: Synthetic progress and applications. *Chem. Sci Eng.* **2014**, *8*, 405–417. [CrossRef]
2. Loudet, A.; Burgess, K. BODIPY dyes and their derivatives: syntheses and spectroscopic properties. *Chem. Rev.* **2007**, *107*, 4891–4932. [CrossRef] [PubMed]
3. Cherumukkil, S.; Vedhanarayanan, B.; Das, G.; Praveen, V.K.; Ajayaghosh, A. Self-assembly of bodipy-derived extended π-systems. *Bull. Chem. Soc. Jpn.* **2018**, *91*, 100–120. [CrossRef]
4. Olivier, J.H.; Barber, J.; Bahaidarah, E.; Harriman, A.; Ziessel, R. Self-assembly of charged bodipy dyes to form cassettes that display intracomplex electronic energy transfer and accrete into liquid crystals. *J. Am. Chem. Soc.* **2012**, *134*, 6100–6103. [CrossRef] [PubMed]
5. Frein, S.; Camerel, F.; Ziessel, R.; Barber, J.; Deschenaux, R. Highly fluorescent liquid-crystalline dendrimers based on borondipyrromethene dyes. *Chem. Mater.* **2009**, *21*, 3950–3959. [CrossRef]
6. Fan, G.; Lin, Y.-X.; Yang, L.; Gao, F.-P.; Zhao, Y.-X.; Qiao, Z.-Y.; Zhao, Q.; Fan, Y.-S.; Chen, Z.; Wang, H. Co-self-assembled nanoaggregates of BODIPY amphiphiles for dual colour imaging of live cells. *Chem. Commun.* **2015**, *51*, 12447–12450. [CrossRef] [PubMed]
7. Tokoro, Y.; Nagai, A.; Chujo, Y. Nanoparticles via H-aggregation of amphiphilic BODIPY dyes. *Tetrahedron Lett.* **2010**, *51*, 3451–3454. [CrossRef]
8. Yang, L.; Fan, G.; Ren, X.; Zhao, L.; Wang, J.; Chen, Z. Aqueous self-assembly of a charged BODIPY amphiphile via nucleation–growth mechanism. *Phys. Chem. Chem. Phys.* **2015**, *17*, 9167–9172. [CrossRef] [PubMed]
9. Cherumukkil, S.; Gosh, S.; Praveen, V.K.; Ajayaghosh, A. An unprecedented amplification of near-infrared emission in a Bodipy derived p-system by stress or gelation. *Chem. Sci.* **2017**, *8*, 5644–5649. [CrossRef] [PubMed]
10. Florian, A.; Mayoral, M.J.; Stepanenko, V.; Fernández, G. Alternated stacks of nonpolar oligo(p-phenyleneethynylene)-BODIPY systems. *Chem. Eur. J.* **2012**, *18*, 14957–14961. [CrossRef] [PubMed]
11. Chen, Z.; Lui, Y.; Wagner, W.; Stepanenko, V.; Ren, X.; Ogi, S.; Würthner, F. Near-IR absorbing j-aggregate of an amphiphilic BF_2-azadipyrromethene dye by kinetic cooperative self-assembly. *Angew. Chem. Int. Ed.* **2017**, *56*, 5729–5733. [CrossRef] [PubMed]
12. Liu, Y.; Zhang, Y.; Fennel, F.; Wagner, W.; Würthner, F.; Chen, Y.; Chen, Z. Coupled cooperative supramolecular polymerization: A new model applied to the competing aggregation pathways of an amphiphilic aza-BODIPY dye into spherical and rod-like aggregates. *Chem. Eur. J.* **2018**, *24*, 16388–16394. [CrossRef] [PubMed]
13. González-Rodríguez, D.; Schenning, A.P.H.J. Hydrogen-bonded supramolecular π-functional materials. *Chem. Mater.* **2011**, *23*, 310–325. [CrossRef]
14. Yagai, S. Supramolecularly engineered functional π-assemblies based on complementary hydrogen bonding interactions. *Bull. Chem. Soc. Jpn.* **2015**, *88*, 28–58. [CrossRef]
15. Rödle, A.; Ritschel, B.; Mück-Lichtenfeld, C.; Stepanenko, V.; Fernández, G. Influence of ester versus amide linkers on the supramolecular polymerization mechanisms of planar bodipy dyes. *Chem. Eur. J.* **2016**, *22*, 15772–15777. [CrossRef] [PubMed]
16. Rödle, A.; Lambov, M.; Mück-Lichtenfeld, C.; Stepanenko, V.; Fernández, G. Cooperative nanoparticle H-type self-assembly of a bolaamphiphilic BODIPY derivative in aqueous medium. *Polymer* **2017**, *128*, 317–324. [CrossRef]
17. Sampedro, A.; Ramos-Torres, A.; Schwöppe, C.; Mück-Lichtenfeld, M.; Helmers, I.; Bort, A.; Díaz-Laviada, I.; Fernández, G. Hierarchical self-assembly of BODIPY dyes as a tool to improve the antitumor activity of capsaicin in prostate cancer. *Angew. Chem. Int. Ed.* 2018. [CrossRef]
18. Sheldrick, G.M. Crystal structure refinement with *SHELXL*. *Acta Cryst.* **2015**, *C71*, 3–8. Available online: http://journals.iucr.org/c/issues/2015/01/00/fa3356/index.html (accessed on 20 November 2018).
19. Sheldrick, G.M. A short history of SHELX. *Acta Cryst.* **2008**, *A64*, 112. Available online: http://http://journals.iucr.org/a/issues/2008/01/00/sc5010/index.html (accessed on 20 November 2018). [CrossRef] [PubMed]
20. Kasha, M.; Rawls, H.R.; El-Bayoumi, M.A. The exciton model in molecular spectroscopy. *Pure Appl. Chem.* **1965**, *11*, 371–392. [CrossRef]

21. Yagai, S.; Tamiaki, H. Synthesis and self-aggregation of zinc chlorophylls possessing an -hydroxyalkyl group: Effect of distance between interactive hydroxy group and chlorin moiety on aggregation. *J. Chem. Soc. Perkin Trans.* **2001**, 3135–3144. [CrossRef]
22. Takasuka, M.; Matsumura, K.; Ishizuka, N. Study of substituent effects on rotational isomers and monomer±dimer equilibria of the 3-carboxy group in 4-substituted (R)-2-(3,4-methylenedioxyphenyl)-6-isopropyloxy-2H-chromen3-carboxylic acids in dilute CCl4 and CHCl3 solutions by FTIR spectroscopy. *Vib. Spectrosc.* **2001**, *25*, 63–79. [CrossRef]
23. Takasuka, M.; Yamakawa, M.; Watanabe, F. F.t.i.r. spectral study of intramolecular hydrogen bonding in thromboxane A_2 receptor antagonist s-l45t and related compounds. Part 1. *J. Chem. Soc. Perkin Trans.* **1989**, 1173–1179. [CrossRef]
24. Choi, S.; Bouffard, J.; Kim, Y. Aggregation-induced emission enhancement of a meso-trifluoromethyl BODIPY via J-aggregation. *Chem. Sci.* **2014**, *5*, 751–755. [CrossRef]
25. Kim, S.; Bouffard, J.; Kim, Y. Tailoring the Solid-State Fluorescence Emission of BODIPY Dyes by *meso* Substitution. *Chem. Eur. J.* **2015**, *21*, 17459–17465. [CrossRef] [PubMed]